

Synthesis of bismuth(III) oxide films based anodes for electrochemical degradation of Reactive blue 19 and Crystal violet

Milica M. Petrović, Jelena Z. Mitrović, Miljana D. Radović, Danijela V. Bojić, Miloš M. Kostić, Radomir B. Ljupković, Aleksandar Lj. Bojić

Department of Chemistry, Faculty of Science and Mathematics, University of Niš, Niš, Serbia

Abstract

The Bi₂O₃ films-based anodes were synthesized by electrodeposition of Bi on stainless steel substrate at constant current density and during different deposition times, followed by calcination, forming Bi₂O₃. The thickness of the films was determined by two methods: the observation under the microscope and by calculation from mass difference. The electrochemical processes at the anodes were investigated by linear sweep voltammetry. At the anodes obtained within 2, 5, 10 and 15 min of deposition, two dyes, namely: Reactive blue 19 and Crystal violet, were decolorized by oxidation with [•]OH radical, generated from H₂O₂ decomposition at the anodes. Decoloration times of the anodes varied, and the shortest one was achieved with the anode obtained during 5 min of deposition, with the film thickness of 2.5±0.3 μm. The optimal H₂O₂ concentration for the dyes degradation was found to be 10 mmol dm⁻³.

Keywords: Bismuth(III) oxide, anodes, synthesis, film thickness, decoloration, hydrogen peroxide.

Available online at the Journal website: <http://www.ache.org.rs/HI/>

SCIENTIFIC PAPER

UDC 544.653.2:547.87-31

Hem. Ind. 68 (5) 585-595 (2014)

doi: 10.2298/HEMIND121001084P

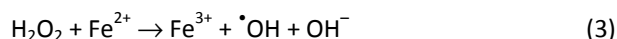
Industry releases huge amounts of more or less colored effluents into the environment. Color itself could be very pernicious to the receiving water sources due to the toxicity towards many aquatic organisms and because colored compounds reduce water transparency, which, in turn, affects photosynthetic activity, thus causing severe damage to the ecosystems [1].

The electrochemical processes for wastewater treatment have many advantages, including: environmental compatibility, versatility, high energy efficiency and safety, because they operate at mild conditions. For these reasons, they have been largely developed and utilized. Among them, the electrochemical oxidation is the most popular electrochemical procedure for removing organic pollutants from wastewaters and it has been widely used for decolorizing and degrading dyes from aqueous solutions. The oxidation of pollutants can be done as the direct anodic oxidation, and direct electron transfer to the anode, which yields poor decontamination; or chemical reaction with electro-generated species from water discharge at the anode surface such as "active oxygen", *i.e.*, hydroxyl radical, [•]OH, which is considered the responsible species for the electrochemical degradation of organic pollutants [2]. Various materials are used as the anodes: Pt [3], boron-doped diamond [4,5], graphite [6] activated carbon fiber [7] and the electrodes based on metal

oxides, such as PbO₂, RuO₂, IrO₂, SnO₂, SbO_x, etc. and their mixtures [8-13]. When hydrogen peroxide is applied to the electrochemical system, the radicals would be electrogenerated with hydrogen peroxide and they would further attack the organic pollutants in the system. In the presence of hydrogen peroxide, both hydroxyl radicals and hydroperoxyl radicals were produced with hydrogen peroxide at the cathode and anode, respectively [14,15]:



The oxidation of organic dyes by hydroperoxyl radicals can be neglected; however, highly reactive hydroxyl radicals produced *via* reaction (1) could react with the organics, resulting in their degradation. In acidic effluents, in the presence of small quantity of Fe²⁺, H₂O₂ decomposes to produce [•]OH and Fe³⁺ [2]:



Generated [•]OH can further decompose the organic molecules.

Anode material is a very important factor determining the extent of decoloration in electrochemical dye degradation processes [2,7,8,12,16-18]. It should possess several important characteristics: an inert surface with low adsorption properties which does not provide catalytically active sites for the adsorption of reactants in aqueous media (providing the formation of high concentration of [•]OH from water discharge), high corrosion stability and high O₂ evolution overvoltage.

Correspondence: M. Petrović, Department of Chemistry, Faculty of Science and Mathematics, University of Niš, 18000 Niš, Serbia.

E-mail: milicabor84@gmail.com

Paper received: 1 October, 2012

Paper accepted: 19 November, 2013

Boron-doped diamond electrodes possess all these properties and they have the highest color removal efficiency [2,4,18]. However, their application at industrial scale is not suitable, mainly due to the difficulties in their preparation and high production cost [2].

Anodes based on metal oxides have high surface area and excellent mechanical and chemical resistance even at high current densities. Various materials based on metal oxides have been used for electrochemical degradation of dyes, showing different color removal efficiency [8–13]. Some semiconductor metal oxide based anodes are used in photoelectrocatalytic processes [2].

Microcrystalline Bi_2O_3 can offer large surface area, electrochemical stability and catalysis behavior [20], which makes it an interesting material for electrochemical oxidation of various organic pollutants. The $\text{Bi}_2\text{O}_3/\text{Ti}$ electrode was used in oxidative degradation of Acid orange 7 by electrolysis, photocatalytic oxidation and photoelectrocatalytic oxidation processes [21]. In addition, Bi_2O_3 is relatively low cost and easy to prepare.

The electrodeposition is a very convenient method of material synthesis, because it is simple and it offers rigid control of film thickness, uniformity, and deposition rate and is especially attractive owing to its low equipment cost and starting materials. In cathodic electrodeposition, the metal ions or complexes are hydrolyzed by electrogenerated base to form oxide, hydroxide, or peroxide deposits on cathodic substrates. Hydroxide and peroxide deposits can be converted to corresponding oxides by thermal treatment [22].

In this work, Bi_2O_3 -based anodes were synthesized by Bi electrodeposition on stainless steel substrate, at constant current density and during different deposition times, followed by calcination. The aim of the work was to investigate the ability of the anodes

obtained during different electrodeposition times to degrade anthraquinone reactive dye Reactive blue 19 and triphenylmethane dye Crystal violet.

EXPERIMENTAL

Materials and equipment

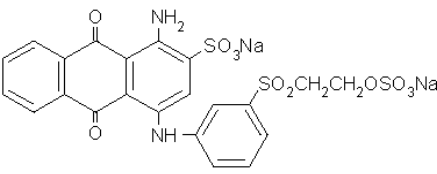
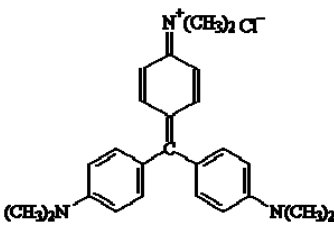
All chemicals were of reagent grade and used without further purification. Bismuth (III) nitrate pentahydrate was purchased from Carlo Erba (Czech Republic), nitric acid, hydrogen peroxide, sodium sulfate; Reactive blue and Crystal violet were purchased from Sigma Aldrich.

All electrochemical experiments were carried out using Amel 510 DC potentiostat (Materials Mates, Italy) furnished with VoltaScope software package. The dye concentrations were determined using UV–Vis spectrophotometer Shimadzu UV-1650 PC (Shimadzu, Japan). Samples were taken during the experiments and their absorbencies were recorded at the wavelengths of 592 nm for Reactive blue 19 and 590 nm for Crystal violet, respectively, at which the dyes show their absorption maxima (Table 1).

Preparation of the anodes

The electrodeposition was performed at room temperature in the two-electrode cell with a stainless steel sheet (10 mm×25 mm) as a substrate for the film deposition (cathode) and Au sheet (10 mm×20 mm) as auxiliary electrode (anode). The distance between working and auxiliary electrode was 15 mm. Before the deposition, the substrate was polished with different abrasive papers, ultrasonically cleaned with ethanol and deionized water. One group of stainless steel samples was anodically treated in 0.5 M oxalic acid at current density of 500 mA cm^{-2} for 30 min. All electrodeposition solutions were prepared with distilled water. 0.1

Table 1. Main characteristics of Reactive blue 19 and Crystal violet dyes

Characteristic	Reactive blue 19	Crystal Violet
Chemical structure		
C.I. generic name	Reactive blue 19	–
Synonym	Remazol Brilliant Blue R	–
IUPAC Name	2-(3-(4-Amino-9,10-dihydro-3-sulpho-9,10-dioxoanthracen-4-yl)aminobenzenesulphonyl)vinyl) disodium sulphate	Tris(4-(dimethylamino)phenyl)methylum chloride
Molar mass, g mol^{-1}	626.54	407.98
λ_{max} / nm	592	590

M Bi³⁺ solutions were prepared by dissolving the required amount of bismuth nitrate in 1 M HNO₃ water solution. The electrodeposition was carried out at constant current density of 40 mA cm⁻² (with regard to geometrical surface area of the stainless steel substrate) with the deposition times of: 1, 2, 5, 10, 15, 30 and 45 min. After the deposition, the electrodes covered with the films were washed with distilled water, dried at room temperature for 24 h, calcined at 500 °C for 90 min in air in a furnace and cooled in the open air. Measurements of the films thickness and the observation of the anodes surfaces were performed using MZ16 A microscope (Leica), equipped with micrometer scale.

In order to perform a more detailed investigation of the obtained material and processes taking place on its surface, another group of the anodes was prepared by electrodeposition under the same experimental conditions as described above, but they were not calcined. Also, following materials were prepared and used as the anodes: a pure stainless steel sheet anodically treated in 0.5 M oxalic acid at current density of 500 mA cm⁻² for 30 min (the same conditions as the substrates for the Bi deposition); and a stainless steel sheet anodically treated in 0.5 M oxalic acid at current density of 500 mA cm⁻² for 30 min and calcined at 500 °C for 90 min in air.

Electrochemical characterization

Characterization of electrochemical processes at the anodes surfaces was performed using linear sweep voltammetry. Voltammograms of the anodes were recorded in the solutions which contained 10 mM H₂O₂ and 1 mM Na₂SO₄ by scanning from 0.6 to 3 V at a scan rate of 20 mV s⁻¹, using saturated calomel electrode as a reference electrode and Au sheet as an auxiliary electrode. The compositions of the solutions were the same as the ones for the dye degradation, but without the presence of the dyes. All the potentials in this work are given versus standard hydrogen electrode.

Dye degradation experiments

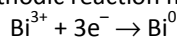
Dye degradation experiments were carried out at room temperature, in two-electrode cell, at constant current density of 10 mA cm⁻², with each of the anodes, using Au sheet as a cathode. Reactive blue 19 and Crystal violet solutions of 50 mg L⁻¹ of the dye, pH 7.0±0.1 and 10 mM H₂O₂ were prepared separately by dissolving the proper amounts of powdered dye and H₂O₂ in water. Each of the solutions contained a 1 mM Na₂SO₄, which provided their electrical conductivity. During the decoloration experiments, the dye solutions were stirred on a magnetic stirrer. Dye decoloration experiments were also carried out using non-calcined bismuth anodes and stainless steel anode. Calcined stainless steel anode was not electrochemically stable enough to be used as the anode; at high potentials

which are applied in our experiments, an intensive corrosion of the anode and oxygen evolution takes place. The decoloration time was observed for each of the anodes. All experiments were performed in triplicate.

RESULTS AND DISCUSSION

All of the films were electrodeposited at the same constant current density, but during the different deposition times. The color of the deposited material was middle gray to pale gray.

For the H⁺ concentration > 0.4 M, which is the case in our work, the Bi³⁺ prevails, and the predominant cathodic reaction may be [23]:



Based on this equation and the color of the deposited films, it can be assumed that bismuth metal was predominantly deposited at the cathode and later, it slowly oxidized in water and air during the drying process.

After the calcinations at 500 °C, the color of the deposited material changed to pale yellow, indicating that the Bi₂O₃ was formed.

Adhesion of the films deposited on the surface which was only treated with abrasives and ultrasonically cleaned, was not satisfying; unlike them, films deposited on the surface which was anodically treated with oxalic acid at high current density had very good adhesion and mechanical stability, which was further improved by calcinations.

Thickness of the films

The thickness of the obtained films was calculated from the mass difference before and after the electrodeposition and calcination, assuming the density of the deposited material was the same as that of the bulk material ($\rho = 9.17 \text{ g cm}^{-3}$ for Bi₂O₃). Note that the thickness determination was performed only for the calcined anodes. Results obtained from this calculation were similar to those obtained by the observation of the cross sections of the stainless steel samples covered with Bi₂O₃ films under the microscope. The differences between the results obtained from these two methods for the current density of 40 mA cm⁻², were between 5 and 20% and they were the lowest for the films with the thickness of about 1.5 to 6 µm. These films were the ones of the highest compactivity and homogeneity. Figure 1 shows dependence of the film thickness of deposition time. Note that the thickness values given in Figure 1 are the ones obtained by observation and measurement under the microscope. The thinnest film, obtained during 1 min of deposition, was quite inhomogeneous, with significantly lower compactivity, and, on some parts of the surface, it could be noted that it wasn't fully formed; its thickness varied a

lot, and it was impossible to measure it with satisfying accuracy, so the thickness value given for it is its calculated value. The films thicker than 12 μm were also inhomogeneous, with larger particles attached to the homogenous part of the film and they were not very stable; when their thickness reached more than 15 μm , they became very unstable and peeled off relatively easily.

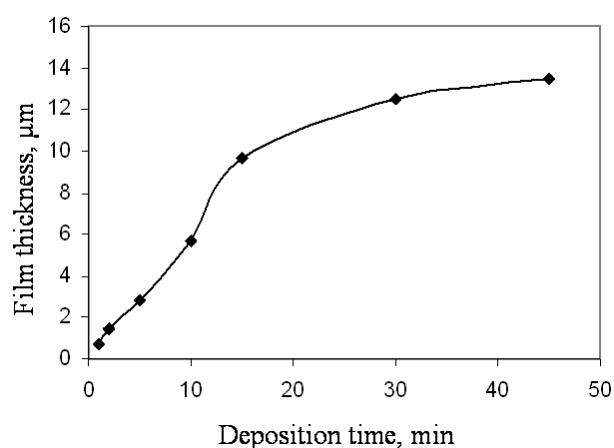


Figure 1. Dependence of the films thicknesses on deposition time.

It can be observed that during the first 15 min of deposition the film thickness rapidly grows with the deposition time. After that time, the film thickness growth becomes significantly slower. Moreover, as mentioned above, the films obtained during the longer deposition times tend to crack and relatively easily peel off, so it can be assumed that the maximum film thickness with the deposition parameters applied in this work was obtained during the first 15–20 min of deposition.

Only the anodes with the film thickness of up to 10 μm were mechanically stable enough to be used in the dye decoloration experiments. The measured thickness values of the films deposited during 2, 5, 10 and 15 min are: 1.5 ± 0.3 , 2.5 ± 0.3 , 5.6 ± 0.5 and 9.6 ± 1 μm , respectively. As mentioned above, the thickness of the film obtained during 1 min of electrodeposition was impossible to measure with satisfying accuracy, so the thickness value given for it is its calculated value of 0.7 μm . In further text, the anodes will be labeled: 0.7, 1.5, 2.5, 5.6 and 9.6, the numbers which correspond to their thickness. The cross section of the anode with 2.5 μm film thickness, which showed the best decoloration results, is presented in Figure 2.

The surfaces of the stainless steel/ Bi_2O_3 anodes are shown in Figure 3.

As it was expected, some differences between the surfaces obtained during different electrodeposition times are observed. During the first minute of depo-

sition (anode 0.7, Figure 3A), a small aggregates have been formed and randomly attached to the surface, leaving a significant part of the metallic surface uncovered. The observation of its cross section confirmed that the Bi_2O_3 film was not fully formed (result is not shown). During the first two minutes (anode 1.5) relatively, the compact layer has been formed (result is not shown), showing that during that time Bi_2O_3 aggregates have covered practically the whole metallic surface (Figure 3B). Though the aggregates are closely packed and well adhered to the metallic surface, the coat that they have formed still appears to be quite porous and not very homogenous on its exposed surface. Surface of the anode 2.5 (Figure 3C) is covered with larger aggregates than anodes 0.7 and 1.5, indicating that between the third and the fifth minute of deposition the aggregates have significantly grown in size. Its surface is also fully covered, though it seems that the layer is little less compact and more porous than that on the anode 1.5. It is, however, also well adhered to the metallic surface, though the exposed surface of the film is inhomogeneous. Surfaces of the anodes 2.5, 5.6 and 9.6 have similar structures (Figure 3C, D and E), meaning that no further growth of the aggregates is observed, but only the growth of the thickness of the film they have formed. The surface coatings on the anodes 5.6 and 9.6 appear to be little more compact than that on the anode 2.5 and, as the measurements have shown, they are thicker as well.

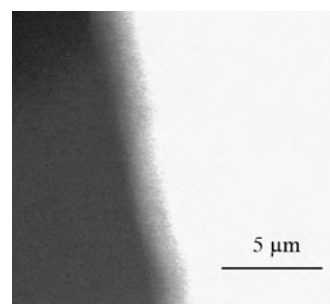


Figure 2. Cross section of the anode with the Bi_2O_3 film thickness of 2.5 μm .

Decoloration of dyes and electrochemical processes at the anodes

Reactive blue 19 is very stable in the solutions used in this work, and it practically does not react with H_2O_2 without electrochemical treatment during the time period of 24 h. The study of Radović *et al.* [24] with the same dye gave the similar results. Crystal violet slowly reacts with H_2O_2 and it takes about 15 h for it to be completely decolorized.

Before the experiments with the calcined anodes, dye decoloration was performed using non calcined bismuth anode and stainless steel anode. All of the experiments were performed under the same decolor-

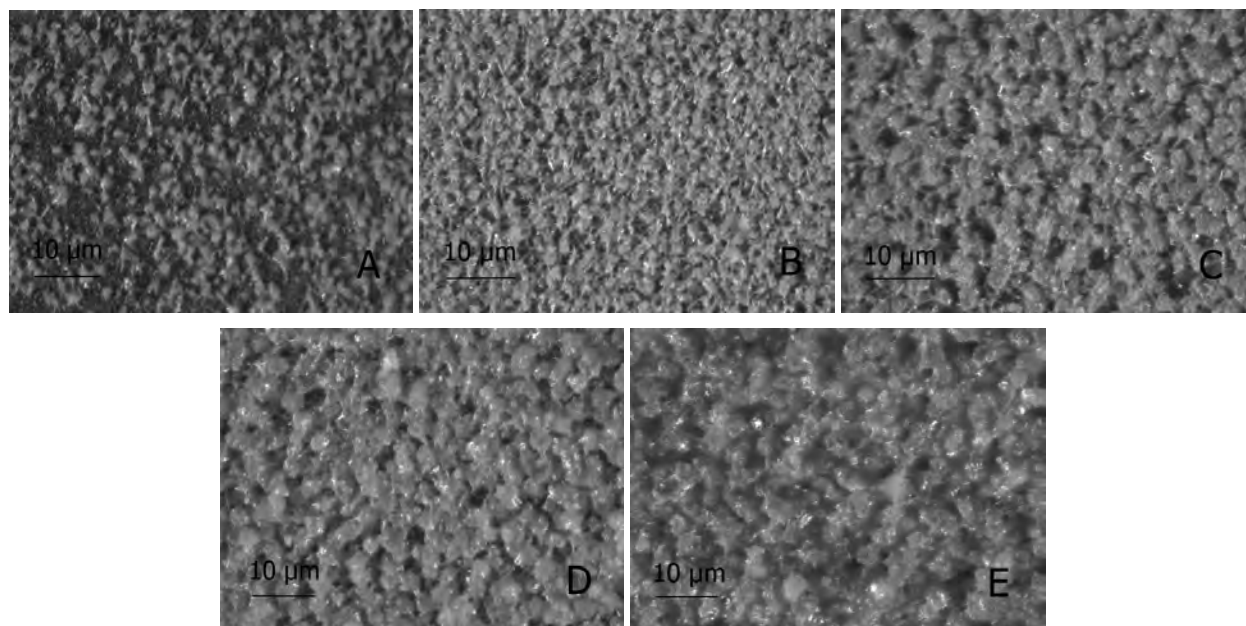


Figure 3. Surface structure of the anodes with the Bi_2O_3 film thickness of: A) 0.7, B) 1.5, C) 2.5, D) 5.6 and E) 9.6 μm .

ation conditions. Non calcined bismuth anodes were not chemically stable under the experimental conditions; they quickly started to corrode during the experiments and the solutions became turbid; after the sedimentation, the precipitate was dissolved in HNO_3 and Bi metal was detected by atomic absorption spectrophotometry (A Analyst 300 (Perkin Elmer, USA)), indicating that the material obtained by electrodeposition was predominantly metal Bi, which was anodically dissolved during the process. With stainless steel anode purple color of Crystal violet and blue color of Reactive blue 19 disappeared within 60 and 130 min, respectively, but the color of the solutions after that time became pale yellowish-green and it has not changed during prolonged electrochemical treatment. Though the solutions looked clear, after 24 h a small amounts of precipitate have been detected; the precipitate from both solutions was dissolved in HNO_3 and Fe was detected by AAS, leading to the conclusion that the dyes were electrocoagulated with iron originating from stainless steel [2]. Decoloration on the calcined bismuth anodes provided clear, completely colorless solutions; though some Pourbaix diagrams show that Bi might exist in some kind of dissolved form at neutral pHs and high potentials [25], neither Fe nor Bi was detected in the solutions, so it can be assumed that the material obtained after the calcination at the stainless steel surfaces was Bi_2O_3 and it was chemically stable under those conditions. However, after dye decoloration with the anode 0.7, iron was found in the solution. This iron probably originates from the parts of the anode surface which were not covered with Bi_2O_3 .

In order to reveal and compare electrochemical processes at different anode materials, a linear sweep

voltammetry investigation was performed in the absence of the dyes. Figure 4 represents current–potential dependence of the stainless steel anode treated in oxalic acid and Bi_2O_3 anode 0.7 in the presence and absence of H_2O_2 , as well as the current–potential dependences of Bi_2O_3 anodes 1.5, 2.5, 5.6 and 9.6 in the absence of H_2O_2 . Figure 5 represents current–potential dependence of Bi_2O_3 anodes 1.5, 2.5, 5.6 and 9.6 in the presence of H_2O_2 .

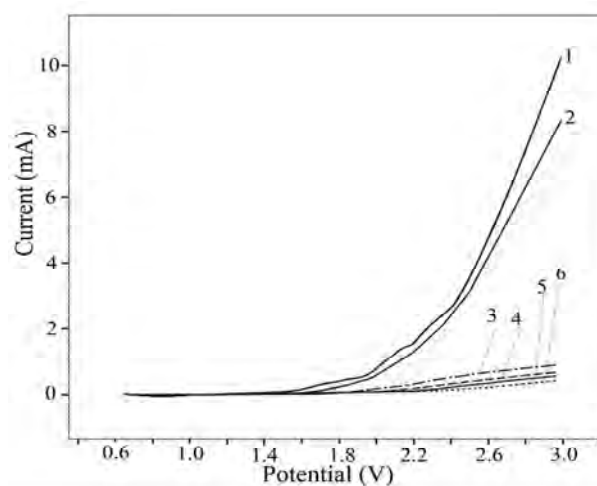


Figure 4. Linear voltammograms of: 1) stainless steel anode in 10 mM H_2O_2 and 1 mM Na_2SO_4 ; 2) stainless steel anode in 1 mM Na_2SO_4 ; 3), 4), 5) and 6): anodes 1.5, 2.5, 5.6 and 9.6, respectively, in 1 mM Na_2SO_4 .

Significant differences in the corresponding lines between stainless steel anode and Bi_2O_3 anodes can be observed. Current–potential dependence of stainless steel anode in the presence of H_2O_2 (Figure 4, line 1)

shows that the current starts to grow at the potential of about 1.50 V. This growth can be attributed to a corrosion of the anode and oxygen evolution. At the potential of 1.95 V current starts to increase more rapidly, with the higher slope of the corresponding line than that between 1.5 and 1.95 V, indicating the beginning of some other electrochemical process. Starting from this potential (1.95 V), the growth of the current is practically linear, and no significant further changes in its shape are observed in the scanned potential region. The current–potential dependence of stainless steel anode in the absence of H_2O_2 (Figure 4, line 2) has very similar shape, with the little lower current values than those in the presence of H_2O_2 . This indicates that similar processes are taking place in the presence and absence of H_2O_2 at this anode. A rapid growth of the current starting from about 2V might be attributed to a formation of ferrate ion, FeO_4^{2-} . This anion can be generated by anodic oxidation of iron and its alloys, with the standard electrode potential of 2.20 V in acidic solutions and 0.72 V in alkaline solutions, respectively [26]. Dissolution of iron can be further confirmed by corresponding Pourbaix diagram, which shows that at neutral pHs and electrode potentials higher than 2V (which is the case in our dye degradation experiments), metallic iron exists mainly as FeO_4^{2-} [27]. Bi_2O_3 -based anode 0.7 has a similar electrochemical behavior as the stainless steel anode in the scanned potential region, in the presence and absence of H_2O_2 (results are not shown). The rapid current increase is observed between 2.2 and 2.3 V, which is a little higher potential than at the stainless steel anode. This difference can be attributed to a different nature of the anodes' surfaces. The observed current is somewhat lower than that obtained with stainless steel anode. Electrochemical behavior of this anode is also similar in the presence and absence of H_2O_2 . This all indicates that at this anode dominant processes are basically the same as those taking place at the stainless steel anode. Having in mind that the dye decoloration times for stainless steel anode and anode 0.7 are very similar (60 min for Crystal violet for both of the anodes and 130 and 110 min for Reactive blue 19 for stainless steel anode and anode 0.7, respectively), it can be assumed that electrogenerated ferrates are responsible for the dyes decoloration at both of these anodes. Current-potential dependences of Bi_2O_3 anodes 1.5, 2.5, 5.6 and 9.6 (Figure 4, lines 5, 6, 7 and 8, respectively) in the absence of H_2O_2 is entirely different than that of stainless steel anode and anode 0.7. No significant current is observed within the scanned potential region. However, starting from about 2.2 V, a low current can be observed. It increases linearly with the increasing potential and no further change in the shapes of the corresponding curves is observed in the scanned potential region. This current is much

lower than the currents that correspond to electrochemical processes taking place at the stainless steel and anode 0.7, as well as at Bi_2O_3 anodes in the presence of H_2O_2 (see below); it is safe to assume that this current cannot be attributed to any particular electrochemical process which might lead to dyes decoloration; no detectable decoloration of the dyes at anodes 1.5, 2.5, 5.6 and 9.6 in the absence of H_2O_2 within 2 h at 10 mA cm^{-2} , 1 mM Na_2SO_4 and 50 mg L^{-1} initial dyes concentration took place. This also indicates that direct dyes oxidation at the anodes did not happen.

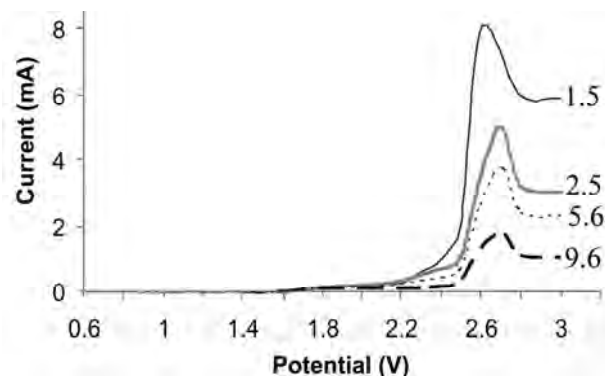


Figure 5. Linear voltammograms of the Bi_2O_3 -based anodes: 1.5, 2.5, 5.6 and 9.6 in 10 mM H_2O_2 and 1 mM Na_2SO_4 .

Figure 5 shows current–potential dependence of Bi_2O_3 anodes 1.5, 2.5, 5.6 and 9.6 in 10 mM H_2O_2 and 1 mM Na_2SO_4 . The shapes of the lines are very different from the ones obtained in the absence of H_2O_2 . At high potentials, H_2O_2 decomposes with the formation of $\cdot\text{OH}$, a very strong oxidant which can oxidize many organic compounds. Standard electrode potential for that reaction is 2.8 V [2,28]. This is very close to the potential values of current peaks at 2.65 V for the anode 1.5 and between 2.74 and 2.78 V for the anodes 2.5, 5.6 and 9.6 in the presence of H_2O_2 (Figure 5). The current peaks values are 8.1, 4.90, 3.76 and 1.85 mA, respectively, which is much higher than the values obtained at the same potentials in the absence of H_2O_2 . Taking into account the potentials of current peaks, and the fact that the dyes decoloration proceeded in the presence of H_2O_2 (see below), these peaks can be attributed to a formation of oxidative species obtained by the decomposition of H_2O_2 at the anodes, probably including $\cdot\text{OH}$, which is responsible for the dye oxidation in this system. All of described electrochemical experiments with Bi_2O_3 anodes in the presence and absence of H_2O_2 were repeated several times and the results were the same, meaning that all the current and potential values were repeatable. No traces of bismuth were detected in any of the solutions after the experiments, including all of the dye decoloration experiments as well. Also, there were no changes in the weight of the anodes before and after the experiments

(the anodes weight was measured before each of the electrochemical experiments, they were cleaned after the experiment and dried at 80 °C for 2 h and then their weight was measured again). This all indicates that the anodes are electrochemically stable in the conditions applied in this work.

The current values in their maxima and after reaching the maxima are different for different anodes and they decrease as the thickness of the anodes increases. Different current values at the same potentials indicate different abilities of the anodes to produce oxidative species by the decomposition of H_2O_2 and this might be attributed to different electrical properties of the anodes. It might have occurred due to differences in their thickness, but the reason might be a different crystalline structure of the deposited Bi_2O_3 films as well: it is known that Bi_2O_3 may appear in several crystalline structures: monoclinic α - Bi_2O_3 , stable at room temperature; cubic fluorite type δ - Bi_2O_3 which exists above 729 °C up to melting point at 825 °C; and two metastable phases, which may occur upon cooling near 650 and 640 °C, respectively: the tetragonal β -phase, and body-centered cubic γ -phase. They usually transform to α -phase upon further cooling to the room temperature [29,30]. These phases have different electrical conductivities; metastable phases have about one order of magnitude higher conductivity than α -phase [31]. Crystalline structure of Bi_2O_3 will certainly depend on the synthesis conditions. In our case, the synthesis parameter that varied for different anodes was the time of bismuth electrodeposition and it is possible that the anodes have different crystalline structures. The differences can be already seen in macroscopic structures of the anodes. The macroscopic surface structure of the anode 1.5 is significantly different from the others; the Bi_2O_3 aggregates at its surface are much smaller (Figure 3). The decomposition of H_2O_2 at this anode is observed at a little lower potential (2.65 V) than at the others (2.74, 2.75 and 2.78 V for anodes 2.5, 5.6 and 9.6, respectively). Anodes 2.5, 5.6 and 9.6 have also exhibited different potentials for decomposition of H_2O_2 and the formation of corresponding oxidative species. Although these differences are very small, they still indicate that the nature and properties of the examined anodes are different. It can also be observed that Bi_2O_3 films of the anodes 5.6 and 9.6 are little more compact than the others, besides the fact that they are thicker (Figure 2). The reason for different electrical behavior of the anodes obtained within different electrodeposition times might be different Bi_2O_3 film thickness of the anodes, but it may also be existence of differences in their crystalline structures. At this point, it is hard to assume how much impact each of these two factors (thickness or crystalline structure of the films) has. It is certain, however, that the change

of electrodeposition time, as the one of the synthesis parameters in this work, brought the significant difference in abilities of the anodes to decompose H_2O_2 and form the corresponding species, which could oxidize the dyes.

Decoloration efficiency of Bi_2O_3 anodes

All of the tested Bi_2O_3 anodes exhibited the ability to decolorize two dyes in the presence of H_2O_2 . It is assumed that the dyes were decolorized by oxidation with the strong oxidants formed by the decomposition of H_2O_2 at the anodes at high potentials. Decoloration experiments were also carried out in the absence of H_2O_2 for both of the dyes, under the same experimental conditions as in its presence; after 2 h of electrolysis, the dyes decoloration was negligible. In order to ensure that the possible corrosion of the stainless steel trough Bi_2O_3 film and formation of electro-Fenton reagent (Fe^{+2}) did not occur (which could also lead to the dye degradation), the Bi_2O_3 films were deposited onto titanium substrate, under the same conditions as with the stainless steel; the decoloration experiments in the presence of anodes with the fully formed films gave very similar results as those with the stainless steel substrate, assuming that, even if the electro-Fenton reaction took place, their effect was negligible.

Figure 6 shows the efficiency of the tested Bi_2O_3 anodes for the decoloration of Reactive blue 19 and Crystal violet. Decoloration efficiency is expressed as decoloration time, *i.e.*, the time needed for 100% decoloration of the dye solutions.

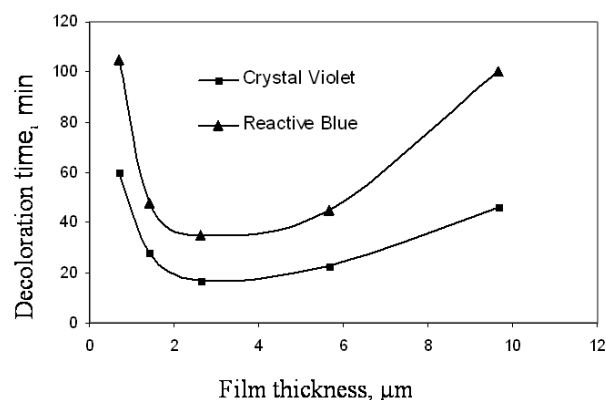


Figure 6. Decoloration times obtained for the anodes with various film thicknesses (initial dye concentration 50 mg dm^{-3} , $10 \text{ mM } H_2O_2$, $1 \text{ mM } Na_2SO_4$, applied current density 10 mA cm^{-2}).

The decoloration times of the anodes significantly differ mutually. Decoloration times of Crystal Violet are shorter than ones of Reactive Blue 19, which can be attributed to the structure, and thus, the stability of the dyes molecules [32]. It can also be observed that two curves have similar shape, which indicates that in

both cases the similar processes are taking place at the anodes surfaces.

As can be seen in Figure 6, the shortest decoloration times, for both of the dyes, are achieved for the anodes with the film thicknesses between 2 and 4 μm ; for the tested anodes, the shortest decoloration time (17 \pm 1 min for Crystal violet and 35 \pm 1 min for reactive blue 19) was achieved for the anode 2.5 (2.5 μm thickness) which was obtained during 5 minutes of deposition. As shown in Figure 5, current values in 10 mM H_2O_2 , attributed to a formation of $\cdot\text{OH}$, are different for different anodes at the same potentials and they decrease as the thickness of the anodes increases from 1.5 to 9.6 μm . Since the dyes are not oxidized directly, but via oxidative species obtained by the decomposition of H_2O_2 , decoloration efficiency of the anodes depends on their ability to produce those species. Based on the current values for the anodes in Figure 5, the abilities of the anodes to decompose H_2O_2 , producing the oxidative species which could degrade the dyes, can be sorted in descending order: 1.5 > 2.5 > 5.6 > 9.6, and, based on that, it is expected that decoloration efficiency decreases in the same way. However, decoloration time of anode 1.5 is longer than that of the anodes 2.5 and 5.6, although it is expected to be able to produce the highest concentration of oxidants that can decolorize the dyes. After decoloration experiments with anode 1.5, the purple and blue shade could be observed at its surface. Desorption of the dyes was performed by immersing the anode in water-ethanol mixture and stirring it for 3 h at 50 $^\circ\text{C}$, and Reactive blue 19 and Crystal violet were detected in the solution, indicating that the dyes adsorbed onto the anode surface and probably blocked the active places for H_2O_2 decomposition. The same experiment was performed with the rest of the anodes, although their color did not visually change; neither Reactive blue 19, nor Crystal violet was detected in the solutions, indicating that dyes did not adsorb onto the other anodes. It can be assumed that anode 1.5 has the highest ability to decompose H_2O_2 , forming the oxidants which oxidized the dyes, but also the highest sorption affinity for the dyes, and that the second prevailed in this case, making it less efficient for decoloration than anodes 2.5 and 5.6.

As already mentioned, the shortest decoloration time was achieved for the anode 2.5. As the film thickness increases from 2.5 to 9.6 μm , the anode's ability to decompose H_2O_2 and form the strong oxidants decreases, and decoloration time slightly increases, as it was expected. The current maxima obtained for the anodes 5.6 and 9.6 were 3.76 and 1.85 mA (Figure 5), which is 77 and 38% of the value obtained for anode 2.5, respectively. Decoloration times of Reactive blue 19 with the anodes 5.6 and 9.6 were 47 \pm 1 and 100 \pm 3

min, which is about 74 and 35% of the efficiency demonstrated with anode 2.5, respectively (having in mind that decoloration time of anode 2.5 for reactive blue 19 was 35 \pm 1 min). Decoloration times of Crystal violet with the anodes 5.6 and 9.6 were 24 \pm 1 and 46 \pm 1 min, which is about 71 and 37% of the efficiency demonstrated with anode 2.5, respectively (having in mind that decoloration time of anode 2.5 for Crystal violet was 17 \pm 1 min). This indicates that decoloration efficiency of these three anodes is determined by their ability to decompose H_2O_2 , producing the reactive species which oxidize the dyes and no side effects are observed, as in the case of anode 1.5. The smallest difference in decoloration times is observed between the anode 2.5 and 5.6, for both of the dyes. As it is shown in Figure 6, for the film thicknesses higher than about 6 μm , the decoloration time significantly increases as well, and greater difference is observed between the anodes 5.6 and 9.6, than between 2.5 and 5.6. It is not certain which phenomenon actually caused those differences. They all have different thicknesses, but, as mentioned before, it is also possible that their Bi_2O_3 films have different crystalline structures.

Decoloration reactions with varying concentrations of peroxide were done with the anode 2.5, which has shown the shortest decoloration times in the presence of 10 mM H_2O_2 . The results are shown in Figures 7 and 8.

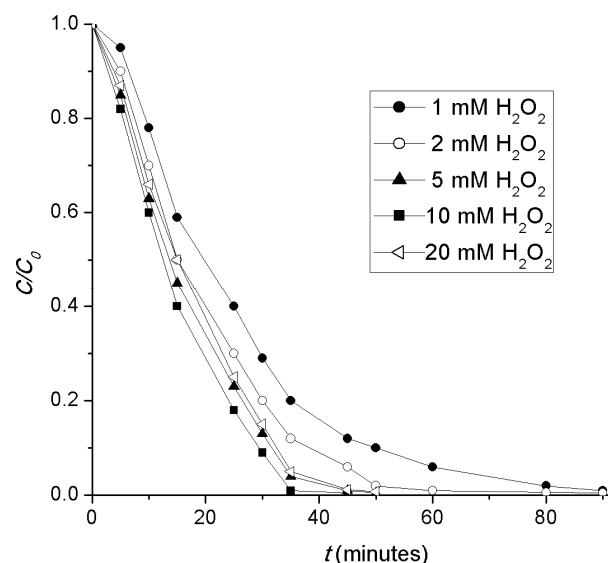


Figure 7. Effect of H_2O_2 concentration on the decoloration time of reactive blue 19 (1 mM Na_2SO_4 , applied current density 10 mA cm^{-2}).

The total decoloration times for reactive blue 19 in the presence of 1, 2, 5, 10 and 20 mM H_2O_2 are: 90, 60, 45, 35 and 45 min, respectively (note that the dye is considered completely degraded when its concentration in the solution is below 1 mass% of its initial concentration). The total decoloration times for Crystal

violet in the presence of 1, 2, 5, 10 and 20 mM H_2O_2 are: 45, 35, 20, 17 and 20 min, respectively. For both of the dyes, for the lower peroxide concentrations (up to 10 mM H_2O_2), the total decoloration time decreases as the peroxide concentration increases, because with the increasing concentration of the peroxide, the concentration of the hydroxyl radicals also increases, as the peroxide is their source. Further increase in peroxide concentration to 20 mM causes the slight decrease in the decoloration time related to that in the presence of 10 mM H_2O_2 , probably because of quenching reaction of hydroxyl radicals with H_2O_2 [24]. Thus, the optimal concentration for the process is assumed to be 10 mmol dm^{-3} .

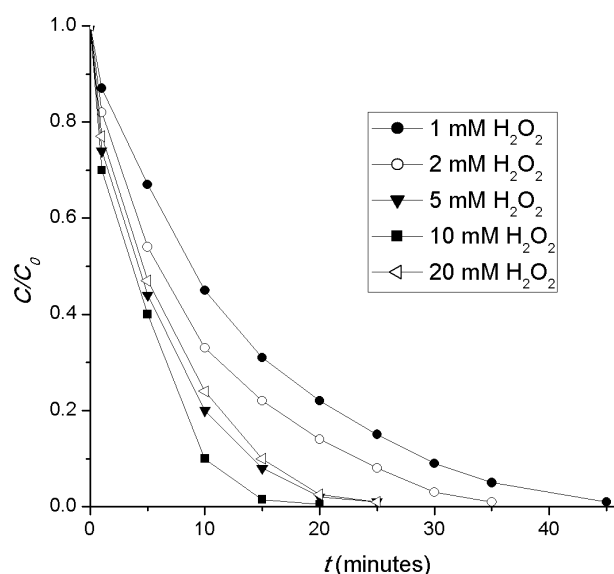


Figure 8. Effect of H_2O_2 concentration on the decoloration time of Crystal violet ($1 \text{ mM Na}_2\text{SO}_4$, applied current density 10 mA cm^{-2}).

All of the dyes degradation experiments were repeated several times, and after each of them, no traces of bismuth were detected in the solutions; the weight of the anodes after cleaning and drying remained constant; no cracks of the films were observed under the microscope, which all indicates that they are electrochemically and mechanically stable enough under the applied experimental conditions. The anodes with the films thicker than $10 \mu\text{m}$ were not tested, because they did not possess required mechanical qualities.

As it is well known, the electrodeposition offers a good control and reproducibility of the working parameters and therefore, the properties of the deposited films; by the proper selection of the electrodeposition conditions, it is possible to obtain material with the desired properties and quality. In this case, it was shown that optimal electrodeposition time in the synthesis procedure was 5 min, *i.e.*, that the anode obtained within this time exhibited the highest effi-

ciency for the dye decoloration under the applied experimental conditions.

Further investigation and optimization of dye degradation parameters will probably improve the efficiency of the process. It would be also interesting to test them as the photo anodes. Since UV irradiation would increase their electrical conductivity and therefore, the production of higher concentration of oxidative species which can degrade the dye molecules their surface, the increase of their efficiency is expected.

CONCLUSION

Bi_2O_3 based anodes were synthesized by electrodeposition of bismuth, followed by calcination to obtain Bi_2O_3 films. The films were deposited at constant current density, during various electrodeposition times, and their thickness varied from about 0.7 to $15 \mu\text{m}$, depending on the electrodeposition time. Only the films with the thickness of up to $10 \mu\text{m}$ were mechanically stable enough to be tested as the anodes. All of the tested Bi_2O_3 anodes have shown the ability to degrade Reactive blue 19 and Crystal violet, with the different decoloration times. Bi_2O_3 film obtained within 1 min of electrodeposition was incomplete, with the significant part of the uncovered stainless steel substrate surface. Dyes decoloration with this anode proceeded through electrocoagulation with anodically generated iron. Dyes decoloration with the rest of the tested Bi_2O_3 anodes proceeded through an oxidation with the oxygen species, which was generated from H_2O_2 decomposition at the anodes surface. The decoloration time of the anode with Bi_2O_3 film of $1.5 \pm 0.3 \mu\text{m}$ thickness was longer than expected, which was attributed to dyes adsorption onto its surface during decoloration process. The shortest decoloration time was achieved with the anode obtained during 5 min of electrodeposition, with the film thickness of $2.5 \pm 0.3 \mu\text{m}$ and this is assumed to be an optimal electrodeposition time in the synthesis procedure of the anodes for the purpose described in the paper. Dye decoloration times increased as the Bi_2O_3 film thickness increased above $2.5 \mu\text{m}$. Effect of H_2O_2 concentration on the dyes decoloration was investigated using the anode with the film thickness of $2.5 \pm 0.3 \mu\text{m}$. H_2O_2 concentration affected the decoloration times. For both of the dyes, the optimal H_2O_2 concentration for the process is found to be 10 mmol dm^{-3} .

Acknowledgement

The authors would like to thank the Ministry of Education, Science and Technological Development of the Republic of Serbia for supporting this work (Grant No TR 34008).

REFERENCES

- [1] M. Doble, A.K. Kruthiventi, *Green Chemistry & Engineering*, Elsevier, Burlington, 2007, pp. 286.
- [2] C.A. Martínez-Huitle, E. Brillas, Decontamination of wastewaters containing synthetic organic dyes by electrochemical methods: A general review, *Appl. Catal., B* **87** (2009) 105–145.
- [3] D. Dogan, H. Türkdemir, Electrochemical oxidation of textile dye indigo, *J. Chem. Technol. Biotechnol.* **80** (2005) 916–923.
- [4] X. Chen, G. Chen, F. Gao, P.L. Yue, High-Performance Ti/BDD Electrodes for Pollutant Oxidation, *Environ. Sci. Technol.* **37** (2003) 5021–5026.
- [5] X. Chen, G. Chen, P.L. Yue, Anodic oxidation of dyes at novel Ti/B-diamond electrodes, *Chem. Eng. Sci.* **58** (2003) 995–1001.
- [6] G. Chen, Electrochemical technologies in wastewater treatment, *Sep. Purif. Technol.* **38** (2004) 11–41.
- [7] W. Chou, C. Wang, C. Chang, Comparison of removal of Acid Orange 7 by electrooxidation using various anode materials, *Desalination* **266** (2011) 201–207.
- [8] J.L. Nava, M.A. Quiroz, C.A. Martínez-Huitle, Electrochemical Treatment of Synthetic Wastewaters Containing Alphazurine A Dye: Role of Electrode Material in the Colour and COD Removal, *J. Mex. Chem. Soc.* **52** (2008) 249–255.
- [9] J.M. Aquino, R.C. Rocha-Filho, N. Bocchi, S.R. Biaggio, Electrochemical Degradation of the Reactive Red 141 Dye on a β -PbO₂ Anode Assessed by the Response Surface Methodology, *J. Braz. Chem. Soc.* **21** (2010) 324–330.
- [10] R. F.Yunus, Y. Zheng, K.G.N. Nanayakkara, J.P. Chen, Electrochemical Removal of Rhodamine 6G by Using RuO₂ Coated Ti DSA, *Ind. Eng. Chem. Res.* **48** (2009) 7466–7473.
- [11] K. Wang, M. Wei, T. Peng, H. Li, S. Chao, T. Hsu, H. Lee, S. Chang, Treatment and toxicity evaluation of methylene blue using electrochemical oxidation, fly ash adsorption and combined electrochemical oxidation-fly ash adsorption, *J. Environ. Manage.* **91** (2010) 1778–1784.
- [12] P.A. Carneiro, C.S. Fugivara, R.F.P. Nogueira, N. Boralle, M.V.B. Zaroni, A Comparative Study on Chemical and Electrochemical Degradation of Reactive Blue 4 Dye, *Portugaliae Electrochim. Acta* **21** (2003) 49–67.
- [13] M. Ihos, F. Manea, A. Iovi, Electrochemical Degradation of Aromatic Compounds at Modified SnO₂ Anodes, *Chem. Bull. Politehnica* **54** (2009) 46–49.
- [14] E. Brillas, E. Mur, R. Saulea, L. Sánchez, J. Peral, X. Domènech, J. Casado, Aniline mineralization by AOPs: anodic oxidation, photocatalysis, electro-Fenton and photoelectro-Fenton processes, *Appl. Catal. B* **16** (1998) 31–42.
- [15] A. Socha, E. Sochocka, R. Podsiadly, J. Sokolowska, Electrochemical and photoelectrochemical degradation of direct dyes, *Color Technol.* **122** (2006) 207–212.
- [16] M. Hamza, R. Abdelhedi, E. Brillas, I. Sires, Comparative electrochemical degradation of the triphenylmethane dye Methyl Violet with boron-doped diamond and Pt anodes, *J. Electroanal. Chem.* **627** (2009) 41–50.
- [17] M. Muthukumar, M. Thalamadai Karuppiah, G. Bhaskar Raju, Electrochemical removal of CI Acid orange 10 from aqueous solutions, *Sep. Purif. Technol.* **55** (2007) 198–205.
- [18] X. Chen, F. Gao, G. Chen, Comparison of Ti/BDD and Ti/SnO₂-Sb₂O₅ electrodes for pollutant oxidation, *J. Appl. Electrochem.* **35** (2005) 185–191.
- [19] G. B. Raju, M. T. Karuppiah, S.S. Latha, D. L. Priya, S. Parvathy, S. Prabhakar, Electrochemical pretreatment of textile effluents and effect of electrode materials on the removal of organics, *Desalination* **249** (2009) 167–174.
- [20] M. Zidan, T.W. Tee, A.I.H. Abdullah, Z. Zainal, G.J. Kheng, Electrochemical Oxidation of Ascorbic Acid Mediated by Bi₂O₃ Microparticles Modified Glassy Carbon Electrode, *Int. J. Electrochem. Sci.* **6** (2011) 289–300.
- [21] G. Li, H.Y. Yip, C. Hu, P.K. Wong, Preparation of grape-like Bi₂O₃/Ti photoanode and its visible light activity, *Mater. Res. Bull.* **46** (2011) 153–157.
- [22] I. Zhitomirsky, Cathodic electrodeposition of ceramic and organoceramic Materials. Fundamental aspects. *Adv. Colloid Interface. Sci.* **97** (2002) 279–317.
- [23] I. Valsiūnas, L. Gudaviėiūtė, A. Steponaviėius, Bi electrodeposition on Pt in acidic medium 1. A cyclic voltammetry study, *Chemija* **16** (2005) 21–28.
- [24] M.D. Radović, J.Z. Mitrović, D.V. Bojić, M.M. Kostić, R.B. Ljupković, T.D. Anđelković, A.Lj. Bojić, Uticaj parametara procesa UV zračenje/vodonik-peroksid na dekolozaciju antrahinonske tekstilne boje, *Hem. Ind.* **66** (2012) 479–486.
- [25] N. Takeno, Atlas of Eh-pH diagrams, National Institute of Advanced Industrial Science and Technology, Tsukuba, 2005, pp. 47.
- [26] M.I. Čekerevac, Lj.M. Nikolić-Bujanović, M.V. Simičić, Istraživanje elektrohemijskog postupka sinteze ferata, deo 1. Elektrohemijsko ponašanje gvožđa i nekih njegovih legura u koncentrovanim alkalnim rastvorima, *Hem. Ind.* **63** (2009) 387–395.
- [27] R.W. Revie, H.H. Uhlig, *Corrosion and Corrosion Control*, 4th ed., John Wiley & Sons, Hoboken, NJ, 2008, pp. 46.
- [28] P.R. Birkin, J.F. Power, M.E. Abdelsalam, T.G. Leighton, Electrochemical, luminescent and photographic characterisation of cavitation, *Ultrason. Sonochem.* **10** (2003) 203–208.
- [29] M. Zdujić, D. Poleti, Č. Jovalekić, Lj. Karanović, Mechanochemical synthesis and electrical conductivity of nanocrystalline δ -Bi₂O₃ stabilized by HfO₂ and ZrO₂, *J. Serb. Chem. Soc.* **74** (2009) 1401–1411.
- [30] H. Cheng, B. Huang, J. Lu, Z. Wang, B. Xu, X. Qin, X. Zhang, Y. Dai, Synergistic effect of crystal and electronic structures on the visible-light-driven photocatalytic performances of Bi₂O₃ polymorphs, *Phys. Chem. Chem. Phys.* **12** (2010) 15468–15475.
- [31] H.A. Harwig, A.G. Gerards, Electrical properties of the α , β , γ , and δ phases of bismuth sesquioxide, *J. Solid State Chem.* **26** (1978) 265–274.
- [32] H. Zollinger, *Color Chemistry: Syntheses, Properties, and Applications of Organic Dyes and Pigments*, 3rd ed., Wiley-VCH, Weinheim, 2003.

IZVOD

SINTEZA ANODA BAZIRANIH NA Bi(III)-OKSIDNIM FILMOVIMA ZA ELEKTROHEMIJSKU DEKOLORACIJU BOJA REACTIVE BLUE 19 I CRYSTAL VIOLET

Milica M. Petrović, Jelena Z. Mitrović, Miljana D. Radović, Danijela V. Bojić, Miloš M. Kostić, Radomir B. Ljupković, Aleksandar Lj. Bojić

Prirodno–matematički fakultet Niš, Univerzitet u Nišu, Niš, Srbija

(Naučni rad)

Anode bazirane na tankim filmovima Bi_2O_3 su pripravljene elektrohemijom taloženjem bizmuta na podlozi od nerđajućeg čelika, pri konstantnoj gustini struje i tokom različitih vremena taloženja i potonjom kalcinacijom do Bi_2O_3 . Debljine filmova su određene dvema metodama: posmatranjem pod mikroskopom sa mikrometarskom skalom i na osnovu razlike u masi. Elektrohemijski procesi na anodama u prisustvu i odsustvu H_2O_2 ispitani su tehnikom linearne voltametrije. Ispitana je sposobnost anoda za obezbojavanje antrahinonske reaktivne boje Reactive blue 19 i trifenilmetanske boje Crystal violet elektrohemijom oksidacijom. Film Bi_2O_3 na anodi dobijenoj u toku 1 minuta elektrotaloženja je bio nepotpun i obezbojavanje na njoj se odvijalo elektrokoagulacijom jonima Fe koji su dobijeni anodnim rastvaranjem nepokrivenih delova površine nerđajućeg čelika. Debljine anoda dobijenih u toku 2, 5, 10 i 15 min elektrotaloženja iznosile su: $1,5 \pm 0,3$, $2,5 \pm 0,3$, $5,6 \pm 0,5$ i $9,6 \pm 1$ μm , redom. Obezbojavanje u prisustvu tih anoda odvijalo se oksidacijom $\cdot\text{OH}$, dobijenim razlaganjem H_2O_2 na anodama na visokim potencijalima. U odsustvu H_2O_2 nije bilo merljivog obezbojavanja. Sve navedene Bi_2O_3 anode su bile mehanički i elektrohemijski stabilne u uslovima obezbojavanja. Sposobnost anoda da generišu $\cdot\text{OH}$ opada s poratom debljine Bi_2O_3 filmova, pa je bilo očekivano da na isti način opada i njihova sposobnost obezbojavanja, tj. da se produžuje vreme obezbojavanja. Ipak, vreme obezbojavanja na anodi debljine 1,5 μm je bilo duže od očekivanog, i ta pojava je pripisana adsorpciji boja na njenoj površini, čime su verovatno blokirana aktivna mesta za generisanje $\cdot\text{OH}$. Na ostalim anodama, debljina 2,5, 5,6 i 9,6 μm nije bilo adsorpcije boja i kod njih su vremena obezbojavanja rasla sa porastom debljine Bi_2O_3 filma, ali se ne može sa sigurnošću tvrditi da je debljina filma glavni uzrok te pojave; verovatno je da i kristalna struktura Bi_2O_3 filmova ima uticaja. Najkraće vreme obezbojavanja postignuto je sa anodom debljine 2,5 μm (17 ± 1 min za Crystal violet i 35 ± 1 min za Reactive blue 19). Vremena obezbojavanja dve boje su bila različita na svakoj anodi, zbog razlike u molekularnoj strukturi boja. Bi_2O_3 filmovi deblji od 10 μm nisu bili dovoljno mehanički stabilni da bi te anode bile testirane. Uticaj koncentracije H_2O_2 na proces obezbojavanja je ispitan na anodi debljine 2,5 μm . Koncentracija H_2O_2 je uticala na vremena obezbojavanja i nađeno je da optimalna koncentracija H_2O_2 u procesu obezbojavanja iznosi 10 mmol dm^{-3} za obe boje.

Ključne reči: Bizmut(III)-oksid • Anode • Sintaza • Debljina filma • Obezbojavanje • Vodonik-peroksid